STRATIFIED FLOW PAST COMPLEX TERRAIN, AND THE PARAMETRISATION OF SUB-GRID-SCALE OROGRAPHIC EFFECTS

Peter G. Baines
CSIRO Division of Atmospheric Research
Aspendale, Australia

Summary

Some salient properties of stratified flow past obstacles are described, with emphasis on wakes and their effect on flow past neighbouring and downstream topography. In the light of these properties, prospects for developing an improved scheme for parametrising the effects of sub-grid-scale topography using cellular automata are assessed, and a possible approach is discussed.

1. INTRODUCTION

Drag of the flow of the atmosphere on the surface of the earth may be loosely divided into frictional boundary-layer drag, and form drag manifested in the surface pressure field. Form drag depends on the properties of inviscid (or more realistically, high Reynolds number) stratified flow past the terrain in question, and is the subject of this paper. Stratified flow past complex terrain has many properties that are not yet fully comprehended. Such flow past a single obstacle is complex enough, involving: (i) gravity wave generation, vertical propagation and eventual dissipation or breaking; (ii) hydraulic transitions and jumps, and (iii) low-level flow splitting, flow separation, wake formation and eddy production. The interaction of these low-level processes with the atmospheric boundary layer does not seem to have been adequately addressed as yet, although we may read more of this in this volume. In complex terrain, topographic features are close enough to influence the flow past the neighbours, or each other. These interactions introduce new phenomena that must be understood and accommodated in order to give a fully satisfying representation of these effects in numerical models.

In this paper we first describe briefly the physical basis for the current scheme used by ECMWF for representing the effects on the atmosphere of flow past topographic features that are too small to be captured by the resolution of the model, known as sub-grid-scale (sgs) topography. The possibilities of improving on this scheme by utilising the mathematical framework of cellular automata are then discussed, and a procedure for progressing in this direction is outlined. In particular, it is necessary to evolve a set of rules for calculating the flow properties in each cell from external considerations and the state of neighbouring cells. The form that these rules must take depends on the nature of stratified flow past the particular

region of topography under consideration, and we may get some feel for the nature of these "rules" by examing such flows. The procedure adopted here is to first describe the character of flow past a single obstacle, and then make some inferences for arrays of obstacles that constitute complex terrain.

2. THE BASIS FOR THE CURRENT PARAMETRISATION

This is described in Chapter 7 of *Baines* (1995) (among other places), and only a brief summary is given here. Practical details, implementation and testing are described by *Lott & Miller* (1997). We consider a grid-point-region (gpr) in an atmospheric general circulation model (AGCM) which may be taken to be 100 km square, and where flow properties within this region are represented by values at the grid point in the centre. The topography is represented by the terms $\overline{h}, \mu, \sigma, \gamma$ and θ, where $\overline{h}$ is the mean height of the whole gpr in the model, μ is the standard deviation of topographic height about this level, σ^2 is the maximum mean square slope, γ^2 is the ratio of the minimum to the maximum mean square slope, and θ is the direction of the maximum mean square slope. From these parameters we may indentify a single obstacle with given height, shape, orientation and lateral extent that, when repeated over the gpr, gives the same values for these parameters for the region. The parameterisation is then based on the properties of the flow past this one particular obstacle. The drag on the atmosphere is manifested in three different forms: gravity wave drag, which may propagate to and manifest itself at great heights, low-level hydraulic flow drag, and low-level separated-wake drag. Each of these forms must be suitably represented in the model.

In general, for stratified flow at speed U and buoyancy frequency N past a mountain of height h, if $Nh/U < 1$ the fluid response is dominated by gravity waves, whereas if $Nh/U > 1$ hydraulic transitions are possible in low-level flow over the mountain, and at low levels the flow splits and passes around the obstacle, causing a separated wake with reduced momentum and possibly, a vortex-street of eddies. Gravity waves are still generated, but from a reduced height of order $(h-U/N)$. Each of these processes causes a drag on the motion of the atmosphere, and these effects may be parameterised separately on physical grounds. Some of these effects are be addressed by other speakers, and particular features of low-level flow are discussed in Sections 5 and 6 below.

Although this approach has been reasonably successful, it has obvious deficiencies. These include the following.

(1) All the topography is represented by one single obstacle shape, whereas in practice there is a distribution of obstacle sizes, heights and shapes in any given gpr.

(2) The effect of the topography is assumed to be distributed uniformly over the whole gpr, whereas the location of the topography may have any distribution.

(3) No allowance is made for the effect of topographic features on flow past its neighbours, and in addition,

(4) no allowance is made for the effect of sgs topography outside the gpr on flow past sgs topography within it.

(5) No allowance has been made for variation of the large-scale flow across the gpr. And also

(6) no allowance has been made for the effect of the Coriolis force on these sgs flows.

Given these omissions it is somewhat surprising that the procedure works at all.

3. CELLULAR AUTOMATA

At the ECMWF workshop of last year, *Palmer* (1996) suggested that cellular automata could be utilised to provide a better framework for parameterising sgs orographic effects (and convection), and in particular that some of the above shortcomings could be avoided with this approach. A cellular automata (CA) model is a system in which each cellular automaton occupies a discrete unit of space, and has a discrete set of values at a discrete set of times. At each time step, the value of the relevant variable in each automaton is updated according to a set of rules that express its relationship to the state values in neigbouring automata at the previous time step (or steps). Most arrays of automata are rectangular (see Figure 1). From a given set of initial conditions, these simple algebraic relations (the rules) determine the subsequent behaviour for the whole system. Despite their intrinsic simplicity, cellular automata with appropriate rules have been shown to represent quite complex systems that operate on larger scales. For example, with relatively simple rules they may represent the Navier-Stokes equations (*Frisch et al.* 1986), and there is now an extensive and rapidly growing literature on them.

4. FORMULATING A NEW SGS OROGRAPHIC PARAMETRISATION SCHEME USING CELLULAR AUTOMATA

In order to apply CAs to the problem in question, we need to first construct an array of cells that cover the gpr. There are many possibilities. For example, the array may be a three-dimensional block, where the topography is enclosed within the three-dimensional array of

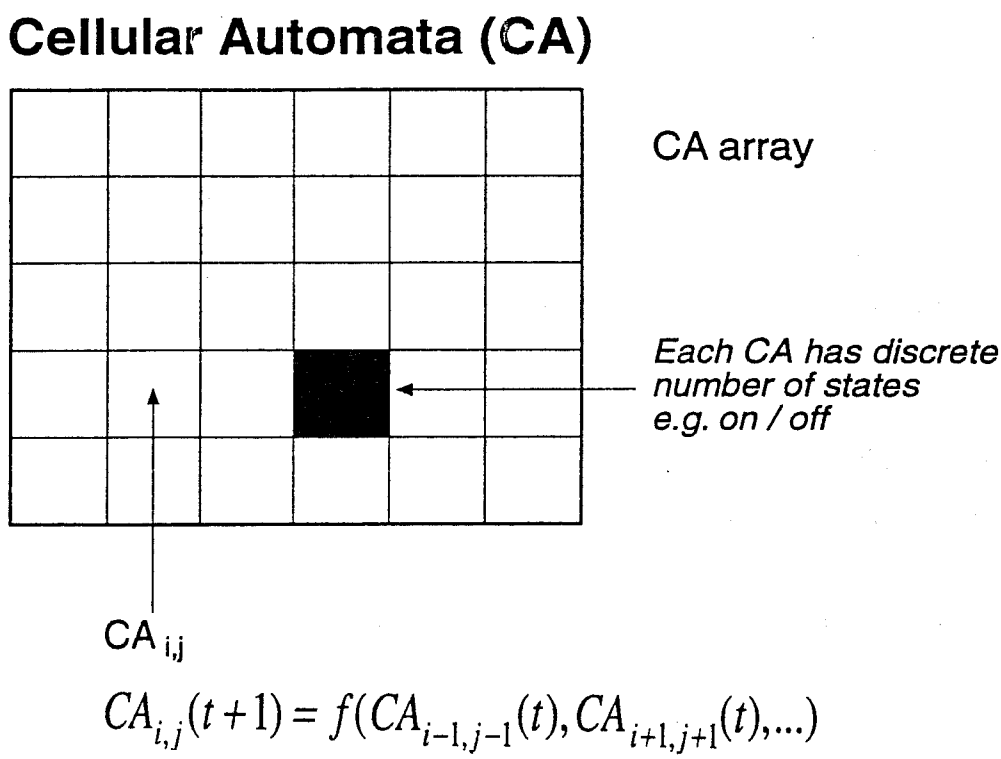

Fig. 1 Cellular automata, or CA, which are variables assigned to given cells in a grid. Each CA has a discrete number of states which for present purposes may be quite large. The value of each CA at each time step depends on values at neigbouring cells at previous time steps, and/or at some cells at the same time step (from Palmer 1996).

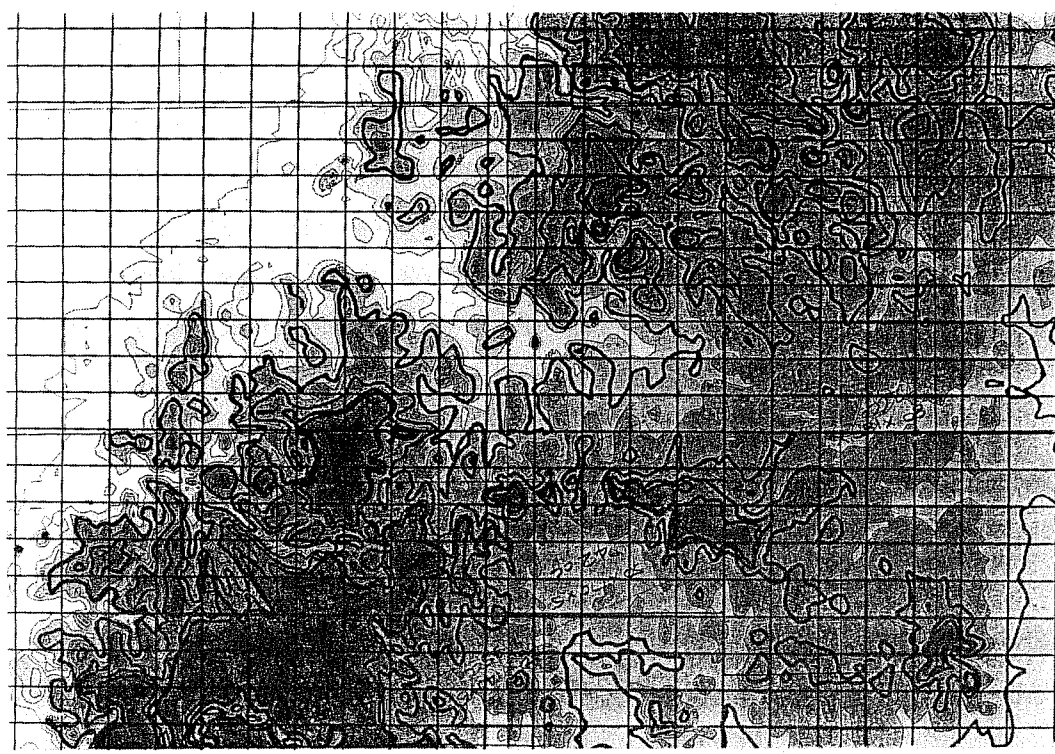

Fig. 2 An array of cells over typical complex terrain (a coastal region of northern New South Wales, Australia). The long side of this diagram is approximately 100 km.

cells. Here, only the cells situated above the topographic surface would be considered. Alternatively, the array could be two-dimensional, as in Figure 2. For present purposes we choose a two-dimensional case where the cells are rectangular in plan view but are situated on the topography, so that each spans a range of heights.

We next consider the drag, or more precisely, the pressure force $P\nabla h$ (where P is the atmospheric pressure), on the topographic surface specified by $z = h(x,y)$, and identify a value P_{ij} that represents the value of P in the cell (i,j). The size of these cells is arbitrary, but obviously determines the scale of resolution being considered, and will depend on a trade-off between the resolution desired and computational time. If we can determine the pressure on each of these cells at a given time step then we know the form drag on the atmosphere (at this resolution). Where this is manifested in the mean flow of the atmosphere is a different question that we will come to presently. The pressure at any cell will depend on:

(i) the overlying external wind field above the gpr;

(ii) neighbouring topography;

(iii) neighbouring small-scale flow (i.e. on the scales of the sgs topography);

(iv) the past history of the flow.

In the cellular automata framework, the value of P_{ij} will depend on a set of rules. In the present context we may ask two questions:

1. What will these rules be like?

2. What is the best way of determining them?

We address the second question first. Here the answer is, probably, by the use of a mesoscale numerical model that is embedded in the large-scale model, and can be related to the chosen cells. This mesoscale model would need to be run for a sufficient number of external wind directions and speeds, in steady-state, with increasing wind speed, with decreasing wind speed, with horizontal shear, etc. However, the rules need not be as complicated as this procedure would suggest, and this leads us to Question 1 and a consideration of the nature of flow past topography. The answer here depends on how the flow past neighbouring cells/topography affects each other. For small cells, this dependency may extend over a large number of neighbours. As shown below, most of this dependency will be centred around the upwind direction for a given cell, and also spread over time. Let us first look at the flow pattern past a single obstacle/mountain, with a view to how this flow may affect the flow over neighbouring topography.

5. FLOW PAST ISOLATED OBSTACLES

As mentioned above, for an isolated single-peaked obstacle the character of the flow depends on Nh/U. If $Nh/U < 1$, (or at least a number close to 1 - there is some dependence on shape) the flow passes over the obstacle and is approximately described by linear perturbation theory. There is some degree of lateral divergence which is suggestive of incipient flow splitting, and the vertical displacement of the flow generates internal gravity waves that propagate upwards and outwards. Here these gravity waves constitute the principal form of drag on the atmosphere. On the lee side of the obstacle, the fluid velocity is almost undisturbed, although at the lowest levels the streamlines diverge laterally as they flow over the obstacle, and remain spread as the flow continues downstream.

For $Nh/U \sim 1$, the low-level flow has an hydraulic character; here the amplitude of the linear solution has increased to the extent that nonlinear terms are now important in the low-level airstream. The precise nature of events depends on the obstacle shape and the form of the airstream. A illuminating example in flow past islands in the Carribean has recently been described by *Smith et al.* (1997). Here the stratification contains the trade wind inversion at a height of about 2.5 km, which is considerably higher than the islands being studied, and below this inversion the flow and conditions give $Nh/U \approx 2$. On the lee side of these islands there is a wake with reduced momentum that extends downstream for many obstacle/island widths (see Figure 3). Any islands that were downstream would clearly be affected by this wake. In the interpretation of the authors, these wakes are caused by the flow over the island beneath the inversion passing through an hydraulic transition, and then through a stratified hydraulic jump over or shortly downstream of the lee side, which results in greatly reduced momentum in the low-level airstream.

Laboratory experiments with $Nh/U > 2$ also show elongated wakes, but these are partly influenced by flow separation in their lower part. The wake contains two elongated recirculating regions with reversed flow close to the centreline (an illustration is given in Figure 4). This flow pattern has a superficial resemblance to homogeneous flow past a right circular cylinder for Reynolds numbers less than 49, as described below.

When $Nh/U >> 1$, the low-level flow (below h-U/N, approximately) splits and passes around both sides of the obstacle (see Figure 5). This has been amply demonstrated in the laboratory, and there are plenty of examples in atmospheric flows past mountains and islands. For the

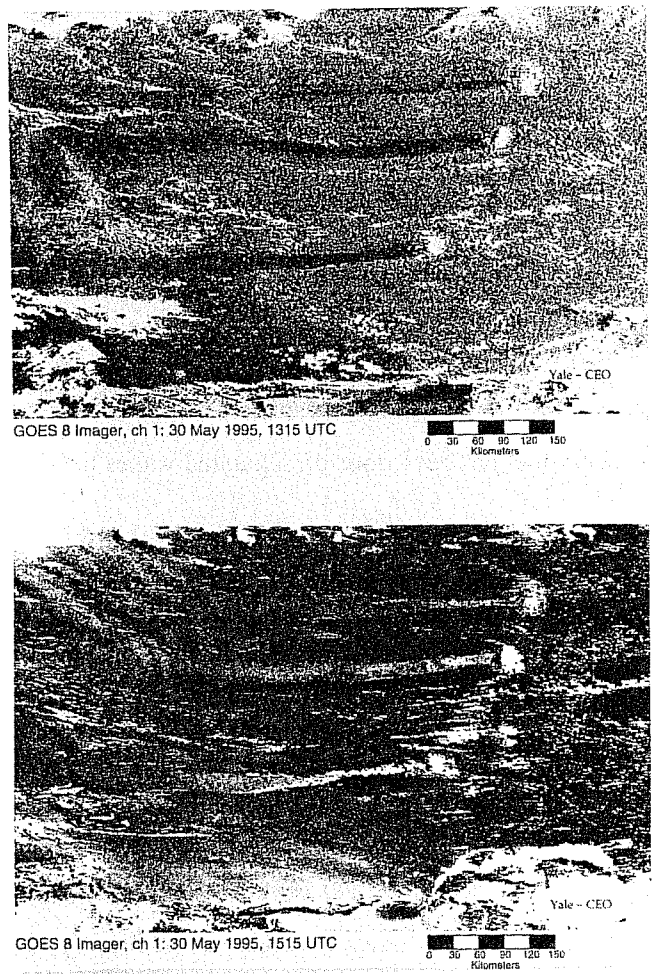

Fig. 3 Wakes of St. Lucia, St. Vincent and Grenada (from top to bottom) in the Windward Islands in the Caribbean, seen from GOES-8 channel-1 (visible) images showing sun glint from the sea surface at two different illumination angles. These images imply reduced sea surface roughness and hence wind speed in the wakes. The second image is brighter because it is closer to the angle for specular reflection (from Smith et al. 1997).

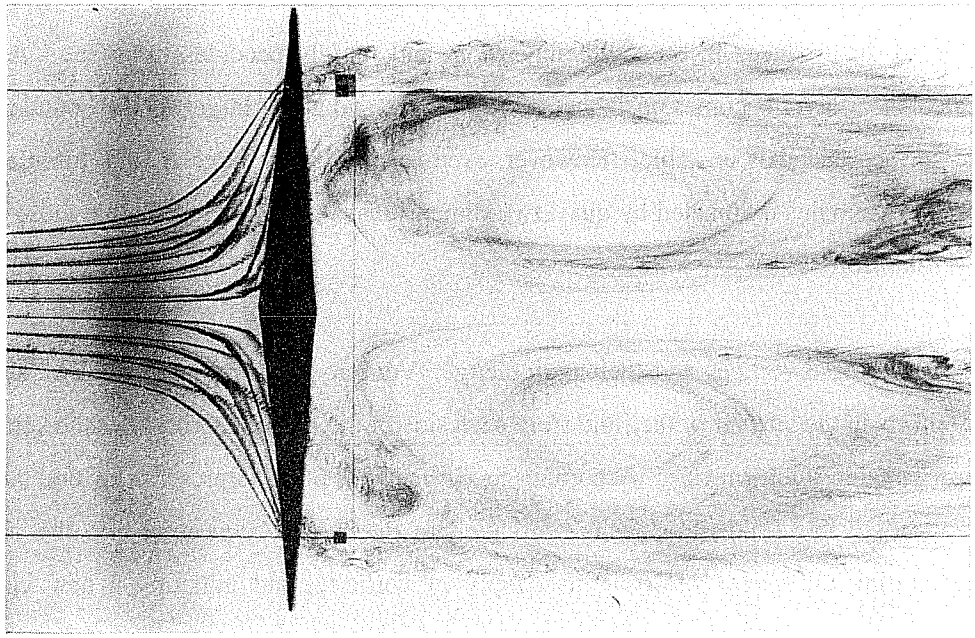

Fig. 4 Plan view of the wake behind a broad, narrow obstacle with $Nh/U = 9.2$, with h = 9.2 cm, width 2A = 114 cm, visualised by dye released from a rake upstream on the left. Note the two elongated counter-rotating eddies, with reversed flow on the centreline. It is likely that given sufficient time, this flow will evolve to a time-dependent vortex street (from Baines 1998).

large Reynolds numbers of these experiments, and in the atmosphere, the flow separates near the lateral extremities, and a broad, extensive wake with reduced momentum (in the mean) results. In the process, vertical vorticity is produced on the upstream side on the surface of the obstacle, and when the flow separates this vorticity is injected, or carried into the body of the fluid. There, some of it "rolls up" to form concentrated vortices and a flow pattern forms that resembles the canonical vortex street in wakes in homogeneous fluids behind circular cylinders (the flow pattern shown in Figure 4 may eventually evolve to reach this stage). In fact, the analogy is sufficiently close to be instructive, and we digress to examine results from the extensive amount of work that has been done on separated wakes behind cylinders.

The flow of homogeneous fluid past a perpendicular circular cylinder (by far the most commonly studied shape) is a function of the Reynolds number, $R_e \equiv UD/\nu$, where U is the mean fluid speed, D is the cylinder diameter (or more generally, the spanwise width) and ν is the fluid viscosity. For $R_e < 49$, after the initiation of motion a symmetric wake consisting of two recirculating regions grows downstream and reaches a steady configuration. Vorticity shed from each side of the obstacle diffuses outward and into the wake, and in the return flow in the eddy, diffuses across the centreline and neutralises with the vorticity of opposite sign in the opposite eddy. The length of this symmetric wake grows linearly with R_e up to the value of 49. In principle there seems no reason why this type of flow may not continue to extend indefinitely downstream with ever increasing R_e, but at $R_e = 49$ the flow becomes unstable (with the character of a Hopf bifurcation) and becomes oscillatory, producing a vortex street. This pattern persists as R_e increases up to 194, but beyond this value the flow becomes unstable to disturbances in the third dimension, and rapidly becomes turbulent. Also, the separated shear layer becomes unstable (see Figure 6), and at yet larger R_e the boundary layer on the surface becomes unstable. However, even for arbitrarily large R_e this turbulent flow (apparently) remains dominated by quasi-two-dimensional vortices that resemble those for $R_e <$ 200 (*Williamson* 1996).

What causes these vortices and their periodicity? Vorticity is being produced and shed into vortex sheets in the interior of the fluid from each side of the obstacle, with opposite sign and at an approximately uniform rate. According to *Gerrard* (1966), the presence of one large lee-side vortex advects fluid of opposite vorticity into the region between it and the obstacle, thereby cutting the vortex off from its supply of vorticity, and initiating a new vortex of opposite sign. The advected vorticity may go in three directions (see Figure 7) - into the

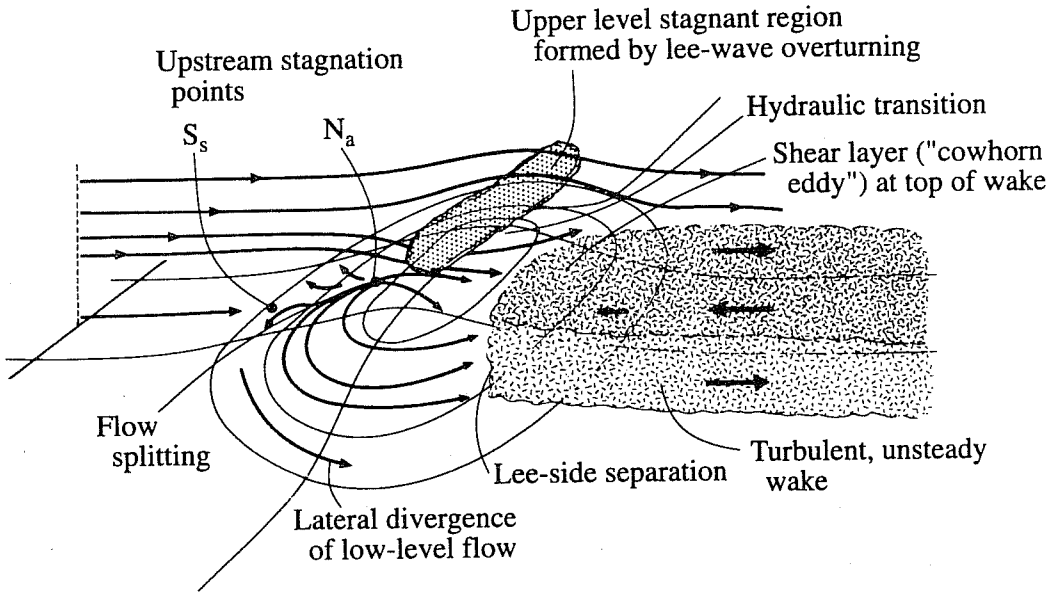

Fig. 5 Schematic diagram of uniformly stratified flow past a symmetric obstacle where Nh/U >> 1. Lines denote streamlines on the surface of the obstacle and in the central plane of symmetry (from Baines 1995).

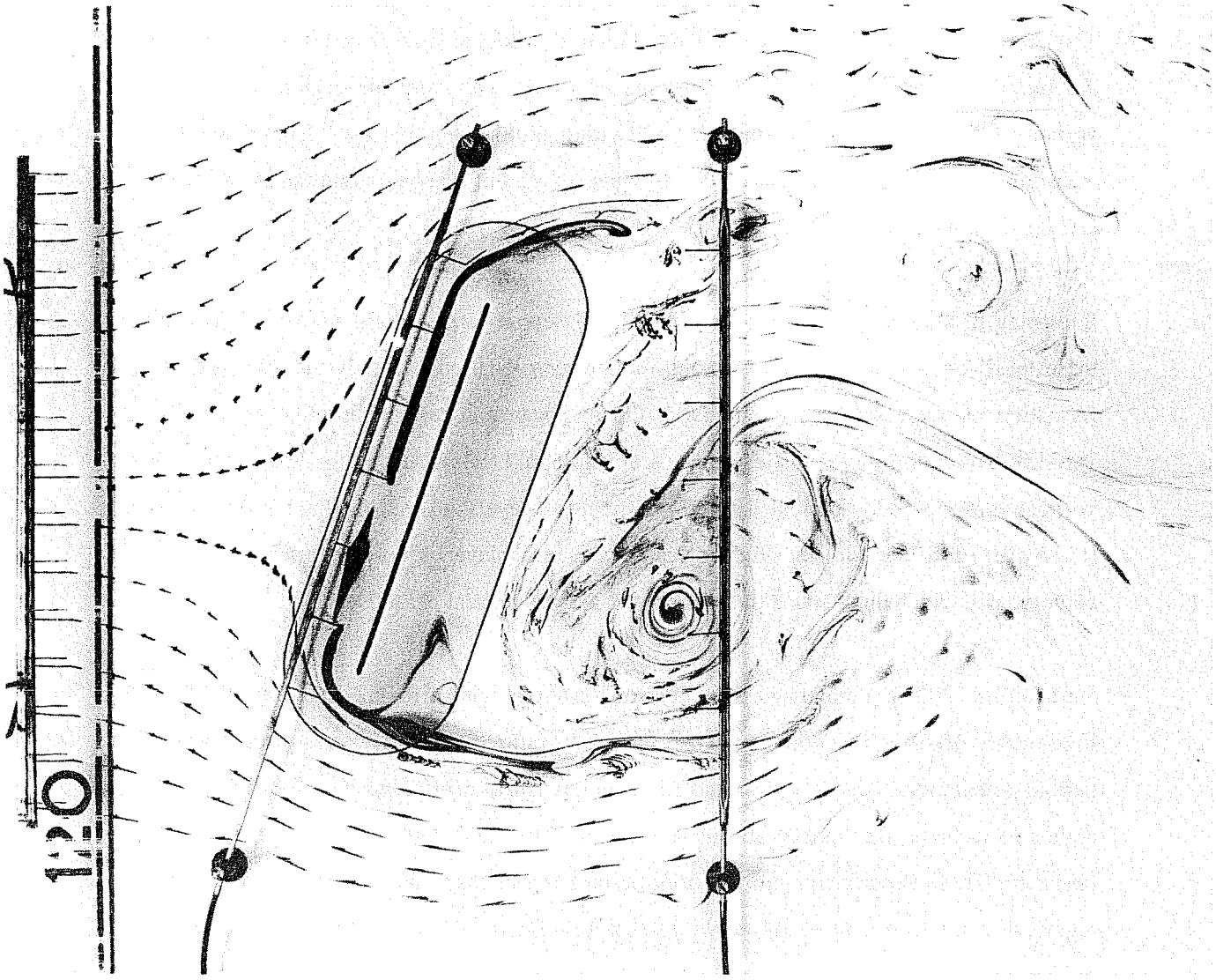

Fig. 6 Observed horizontal flow pattern at a height $z = h_m/3$, for uniformly stratified flow past an angled towed barrier, where h_m is the maximum height of the barrier. $Nh/U = 10$, $R_e = 2990$. Dye is released by three rakes: one upstream, one on the upstream side of the surface of the obstacle, and one in the wake region. The wake region is unsteady, with vortices of opposite sign being shed alternately (photo by the author).

original vortex (of opposite sign), reducing its magnitude, into the region connecting it to its source, neutralising the supply, or into the region immediately behind the obstacle, initiating a new eddy. A time-dependent topology of this process has been described by *Perry et al.* (1982) - see Figure 8.

The shedding frequency for the shedding of vortices on one side is specified by the Strouhal number $St = nD/U$, where n is the shedding frequency in radians/sec. For a circular cylinder, observations show that $St \approx 0.2$, over a wide range of R_e. The period of vortex shedding is then $T \approx 5U/D$. The rate of production of vorticity (of each sign) is 0.5 U_s^2, where U_s is the velocity at the separation point outside the boundary layer. If we take $U_s = 2U$, the amount of vorticity shed in each period, or the total circulation, is $10UD$. However, the magnitude of the circulation in the vortices is observed to be only $(0.5\text{-}1.0)\pi UD$ (e.g. *Green & Gerrard* 1993), so that most of the shed vorticity is mutually annihilated in the regions between the vortices. The nature of the wake can be altered dramatically if artifacts such as centreline splitter plates are introduced downstream, which have the effect of separating the regions of fluid with vorticity of opposite sign, and thereby preventing mutual annihilation. These quantitative measurements have been made at moderate values of R_e, but it appears that the same processes also apply at very large R_e.

Returning to the stratified flow case of low-level flow at large values of Nh/U, the flow at these levels on isentropic surfaces is quasi-two-dimensional and visually the flow and vortex formation on these surfaces is similar to the homogeneous case. Visually, the process of vorticity advection by pre-existing eddies seems to apply. However, at the levels where these vortices form, the eddy periodicity is the same at all levels, so that they are in fact coupled (*Castro et al.* 1983, *Baines* 1998). The flow at each level is not independent, but varies continuously with height, and is three-dimensional with vertical phase lag.

Smith et al. (1997) summarised their field observations with a regime diagram as shown in Figure 9a. A series of laboratory experiments of stratified flow past an isolated obstacle at various orientations, towing speeds and consequently Nh/U values, has been carried out by the author to examine the variety of wakes obtained. The same four types of wake flow were observed. These experiments are far from definitive, but they do suggest a slightly different regime diagram from that of Figure 9a, as shown in Figure 9b. The boundaries between these regimes are vague, and there is more of a continuous transition between these various flow

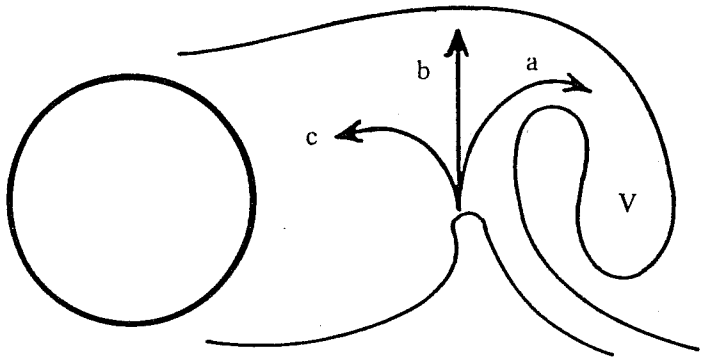

Fig. 7 The process of vortex shedding and cut-off behind a cylinder at large R_e. Vortex V advects vorticity of opposite sign across the region between it and the cylinder, and this advected vorticity may take one of three paths. Path (a) weakens the initial vortex, path (b) neutralises the vorticity feeding it, and path (c) initiates or contributes to a new vortex of opposite sign in the lee of the cylinder (from Gerrard 1966).

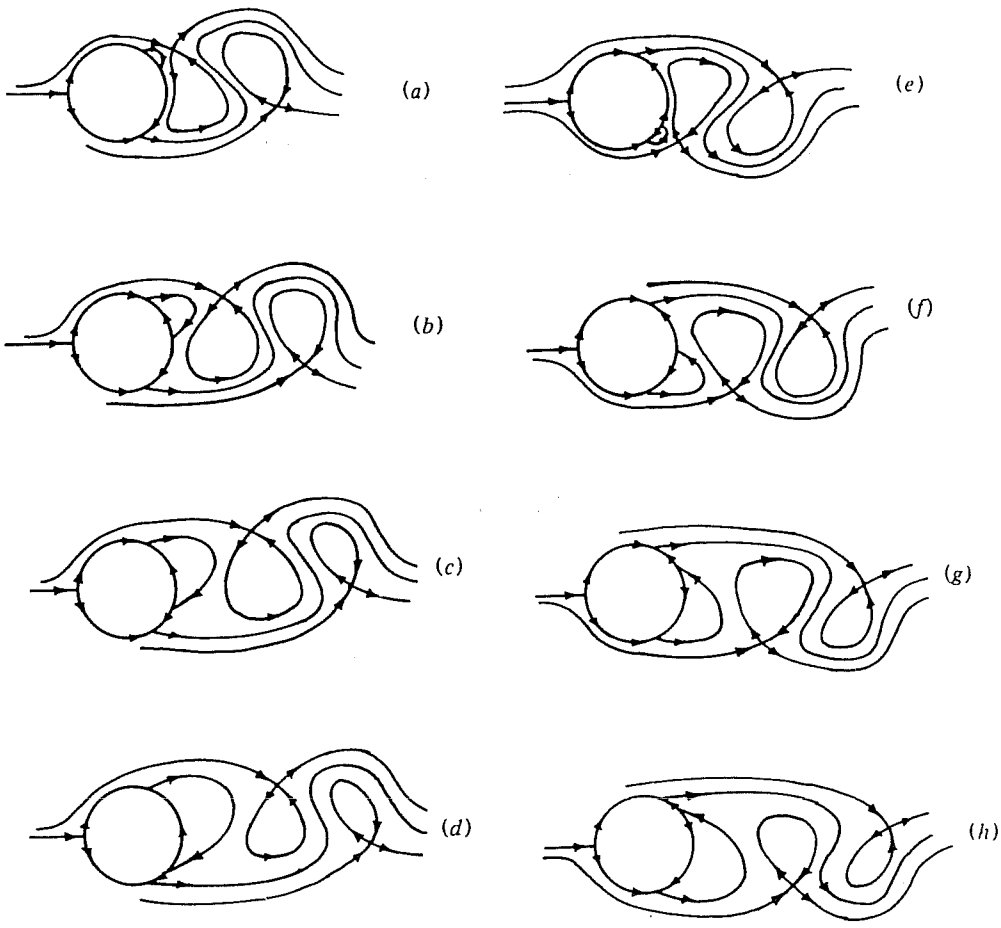

Fig. 8 Instantaneous streamlines at successive times, based on observations, showing the flow pattern in the lee of a cylinder during vortex shedding. The observer is moving with the cylinder, and the time sequence is from (a) to (h) covering half a period (from Perry et al. 1982).

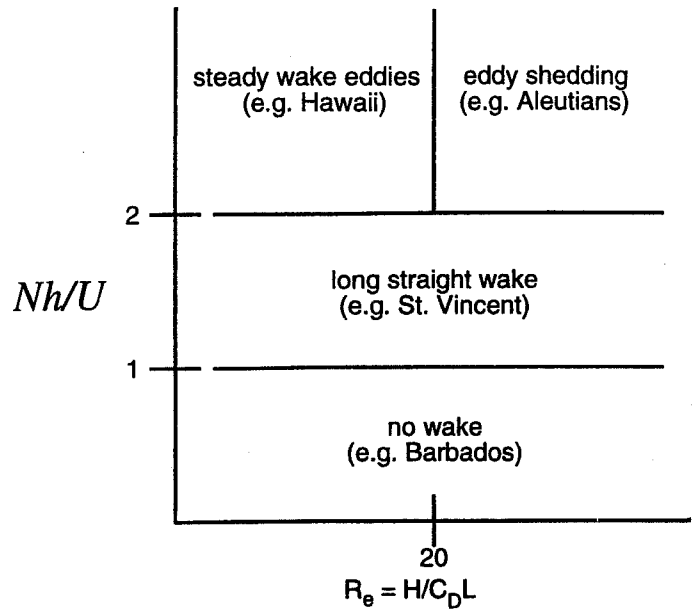

Fig. 9 (a) Wake regime diagram from Smith et al. (1997), suggested by atmospheric observations. The abscissa indicates no variation with a parameter h/C_DL, where C_D is a drag coefficient, and L an obstacle width.

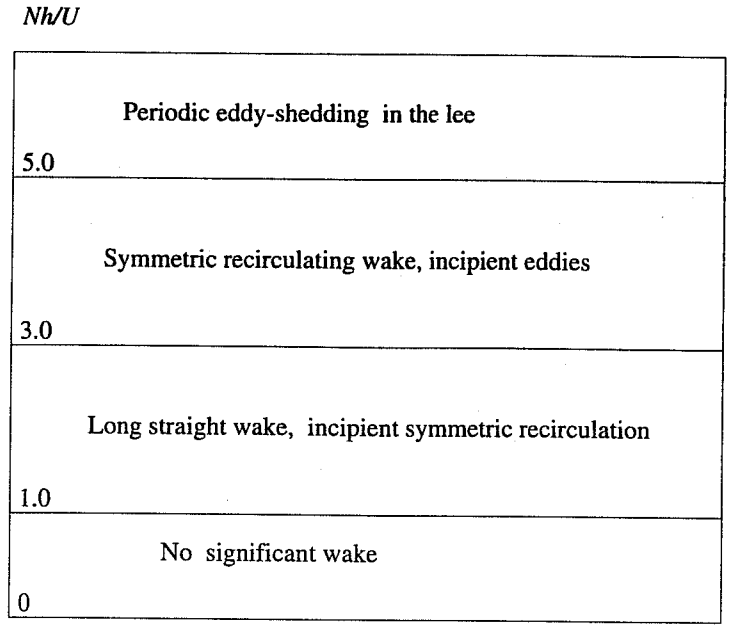

Fig. 9 (b) Corresponding diagram suggested by laboratory experiments. The symmetric wake is shown in Figure 4, and periodic eddy shedding in Figure 6.

types, with the "long straight wake" shortening to give the recirculating regions as Nh/U increases. Oscillations in the wake appear downstream of the recirculating regions, and the oscillations grow *in situ* to form vortices. For larger Nh/U, the symmetric recirculating region shortens, and the eddies form closer to the obstacle. Laboratory experiments have the advantage that the key parameters may be varied at will, but have shortcomings in that the aspect ratios (h/L, where L is the obstacle width) are too large. Never-the-less, the comparisons look quite realistic.

The strength of the wake and the features in it are observed to decay with distance and time downstream, leaving fossilised or frozen features in the Lagrangian dye tracers. This is due to vertical diffusion of momentum from the overlying fluid stream, and frictional drag from the rigid lower boundary. One may obtain an estimate of the time scale involved by considering a prototype diffusion problem, of a two-dimensional (x-z) slab of vertical thickness d, moving at uniform initial velocity U over a solid horizontal boundary, with fluid at rest above. This moving slab represents the wake, and its motion decays with time due to vertical diffusion of momentum. The solution is given by *Carslaw & Jaeger* (1959), and is

$$\frac{u}{U} = 1 - 1.5\,\mathrm{erfc}(X) + 0.5\,\mathrm{efrc}(3X),$$

where $X = d / 4(\nu t)^{1/2}$, $\mathrm{erfc}(X) = \frac{2}{\pi^{1/2}} \int_X^\infty e^{-t^2} dt$, is the complementary error function and ν is the kinematic viscosity. To relate this to the atmosphere, we must replace ν by a vertical momentum transfer coefficient, K_v. This solution shows that the decay of the motions (such as eddies) in the wake, and the wake relative to the surrounding flow, is substantial for times $t > d^2/4K_v$, and for distances $L = Ut > d^2/4K_v$. Although the cutoff is far from sharp, this gives a measure of the downstream influence of topography.

6. FLOW PAST COMPLEX TERRAIN

Briefly, there are many complex possibilities in patterns of low-level stratified flow ($Nh/U >> 1$) around arrays of obstacles. Downstream obstacles may lie within the wakes of obstacles that are upstream, or alternatively, the whole wake may be deflected sideways around a downstream obstacle. The effect of wakes depends on the history of the flow as well as on geometry and the current flow state. Further studies are necessary in order to be able to infer some qualitative principles. Some visual examples illustrating these points are available.

7. DISCUSSION AND CONCLUSIONS

From these considerations we may infer some general ground rules for wakes and downstream regions of topographic influence, as follows.

(i) Wakes grow downstream with time, at the advection speed.

(ii) The character of the wake depends on Nh/U - it is elongated for $1 < Nh/U < 3$, periodically eddy shedding if $Nh/U >> 1$.

(iii) Shed vorticity promotes the generation of eddies unless it is neutralised, and these eddies may form a significant part of the wakes. If vorticity neutralisation is prevented (by downstream topography), the vorticity remains in the flow and may have important consequences downstream.

(iv) The wakes and their structural features decay with time due to vertical diffusion of momentum from above, in a distance scale of order $Uh^2/4K_v$.

We finish by returning to Question 1 - what will the cellular automata rules for the surface pressure field be like? On the basis of the above we may now make some inferences. Let us suppose that the wind commences from rest, and blows from one particular direction at uniform speed for a given period of time that exceeds several time steps in the model. Let us also suppose that there is no significant topography upstream of the gpr in question (e.g. an onshore wind for a gpr bordering a coastline). For the first row of cells the rules will depend only on local topography, and have no history. For downstream points, the values of P_{ij} will depend on the history of the flow, and also on the values of the points upstream. There is a general directional dependence of the cell properties, and a fading memory with time.

This "procedure" will give a distribution of drag on the topography, which covers a range of heights centred on the mean level, $\overline{h}$. One may then proceed by simply summing the drag at each level, and splitting this into the three components (gravity waves, hydraulic and separated wake) in a similar manner as before. There is the additional complexity of representing the effect of the drag on the flow below the level of $\overline{h}$ - the flow in the valleys - in the model. This is real drag, but may be small, since velocities are relatively small there. But the potential exists to do better. A typical gpr has a distribution of topographic heights, and gravity waves may be generated by flow at different levels at different places. There is scope for treating each small scale topographic region individually, with care, in a reasonably economic fashion.

For example, cells near the top of an orographic region may be associated with gravity wave drag, which can possibly be characterised by a representative pressure pattern, whereas for another orographic region of lower height the whole region may be a source of gravity waves, on different length scales.

These considerations may be seen as a starting point towards a new and more ambitious scheme, and the next step may be to work toward some tests with simple scenarios and landscapes.

References

Baines, P.G., 1995: Topographic Effects in Stratified Flows, Cambridge University Press, 482 pp.

Baines, P.G. 1998: Momentum exchange due to internal waves and wakes generated by flow past topography in the atmosphere and lakes. In "Physical Processes in Lakes and Oceans", J. Imberger, ed., Amer. Geophys, Union, to appear.

Carslaw, H.S. & J.C. Jaeger 1959: Conduction of Heat in Solids, Oxford University Press, 510 pp.

Castro, I.C., W. Snyder & G.L. Marsh, 1983: Stratified flow over three-dimensional ridges. J. Fluid Mech. **135**, 261-82.

Frisch,U., B. Hasslacher, & Y. Pomeau, 1986: Lattice gas automata for the Navier Stokes equations, Phys. Rev. Let. **56**, 1505-1508.

Gerrard, J.H., 1966: The mechanics of the formation region of vortices behind bluff bodies. J.Fluid Mech. **25**, 401-13.

Green, R.B. & J.H.Gerrard, 1993: Vorticity measurements in the near wake of a circular cylinder at low Reynolds numbers. J. Fluid Mech. **246**, 675-91.

Lott, F. & M.J. Miller, 1997: A new subgrid-scale orographic drag parametrisation: Its formulation and testing. Q.J. R. Meteor. Soc. **123**, 101-127.

Palmer, T.N. 1996 On parametrising scales that are only somewhat smaller than the smallest resolved scales, with application to convection and orography. Proc. ECMWF Workshop on Convection.

Perry, A.E., M.S. Chong & T.T. Lim, 1982: The vortex shedding process behind two-dimensional bluff bodies. J.Fluid Mech. **116**, 77-90.

Smith, R.B., A.C. Gleason, P.A. Gluhosky & V. Grubišic, 1997: The Wake of St. Vincent. J. Atmos. Sci. **54**, 606-623.

Williamson, C.H.K., 1996: Vortex dynamics in the cylinder wake. Ann. Rev. Fluid Mech. **28**, 477-539.